

# FIRST COMMISSIONING OF LCLS-II CW INJECTOR SOURCE\*

F. Zhou<sup>+</sup>, C. Adolphsen, A. Benwell, G. Brown, W. Colocho, Y. Ding, M. Dunning, K. Grouev, B. Jacobson, X. Liu, T. Maxwell, J. Schmerge, T. Smith, T. Vecchione, F. Wang, C. Zimmer  
 SLAC, Stanford, CA, USA

G. Huang, F. Sannibale, LBNL, Berkeley, CA, USA

## Abstract

The LCLS-II injector source includes a 186 MHz CW rf-gun, a 1.3 GHz CW rf-buncher, a loadlock system for photocathode change, two main solenoids, and a few essential diagnostics. The electron beam is designed to operate at a high repetition rate, up to 1-MHz. Since summer of 2018 we started LCLS-II injector source commissioning immediately after the major installation was completed. Initial commissioning showed the rf-gun was severely contaminated with hydrocarbons and very limited power <600W could be fed into the gun cavity. After a few significant processes, we eventually removed the hydrocarbons and successfully delivered desired rf power of 80 kW to the gun. This paper reports first commissioning results including gun bakeout and vacuum processing, CW RF-gun and buncher operation with nominal power, and measurements of rf stability and dark current.

## INTRODUCTION

LCLS-II currently under construction at SLAC National Accelerator Laboratory is a continuous wave (CW) x-ray free electron laser (FEL) user facility driven by a 4 GeV superconducting (SC) linac [1]. To meet the x-ray FEL requirements, the LCLS-II injector must simultaneously deliver high repetition rate up to 1 MHz and high brightness electron beam with normalized emittance of <0.4  $\mu\text{m}$  at nominal 100 pC/bunch and peak current of 12 A. The major beam requirements for the LCLS-II injector are summarized, as given in Table 1.

Table 1: Major LCLS-II Injector Beam Requirements

Parameter	Nominal
Gun energy (keV)	750
Bunch repetition rate (MHz)	0.93
Bunch charge (pC)	100
Peak current (A)	12
Slice emittance ( $\mu\text{m}\cdot\text{rad}$ )	0.4

Figure 1 shows the schematic layout of the LCLS-II injector source, which includes one 186 MHz CW normal conducting (NC) rf-gun, one 1.3 GHz 2-cell CW NC rf-buncher for compressing the bunch length, two solenoids for the focusing, and five pairs of steering correctors for measuring the electron beam energy and beam steering. Diagnostics include two BPMS, one YAG screen, one current monitor ICT and a temporary Faraday cup (FC) for measuring the absolute bunch charge. The FC will

eventually be removed before connecting the  $\sim 1$  MeV injector source to the first 100-MeV cryomodule.

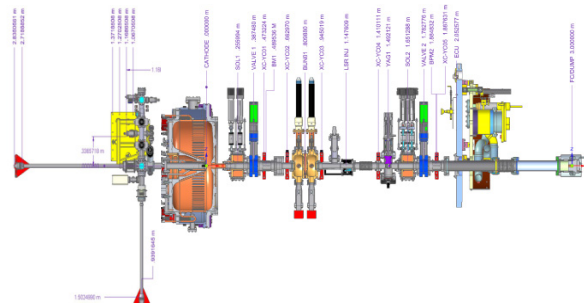


Figure 1: Schematic of the  $\sim 1$  MeV LCLS-II CW injector source under commissioning.

## FIRST COMMISSIONING RESULTS

The LCLS-II RF gun and buncher were made by LBNL [2, 3], and installed by SLAC. Since summer of 2018, we started commissioning for the gun and buncher.

### RF Gun Bakeout

The original plan was to bakeout the large rf-gun with an average 3-4 kW of rf power. But only <600 W peak power could be fed into the gun cavity due to the strong multipacting effect caused by severe hydrocarbons contaminations in the gun from oil contamination in the NEG pumps. Figure 2 shows one example of forward and reversed power waveforms when multipacting happens.

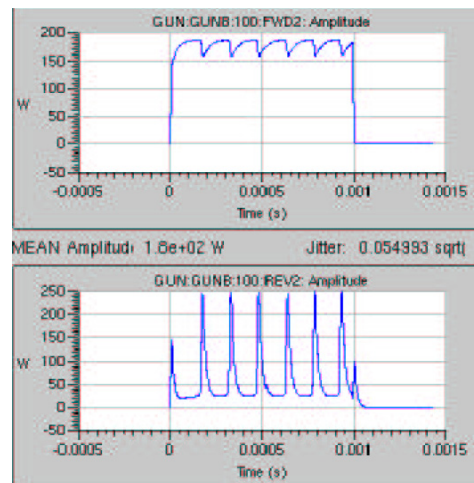


Figure 2: Forward (top) and reversed (bottom) rf power waveforms due to multipacting.

We changed strategy from an rf to a thermal bake and baked the gun up to 190°C for >10 days but no notable

\* Work supported by US DOE under grant No. DE-AC02-76SF00515  
 + zhoufeng@slac.stanford.edu

Content from this work may be used under the terms of the CC BY 3.0 licence (© 2019). Any distribution of this work must maintain attribution to the author(s), title of the work, publisher, and DOI

improvement on the hydrocarbons and multipacting was seen. A long period of conditioning followed by a special slow activation of the NEG's significantly reduced the hydrocarbon partial pressure and improved the gun vacuum pressure. The improved vacuum pressure also eliminated the multipacting and allowed full 80-kW of rf peak power delivery to the gun cavity.

### Further Gun Vacuum Improvement

The static gun vacuum was  $7e-11$  Torr but with rf on at nominal average power the vacuum increases to about  $2e-8$  Torr. The gun vacuum was then improved to  $6.5e-9$  Torr, as shown in Fig. 3, after sixteen hours of continuous rf power processing with nominal power. We noted the outgassing comes from the coaxial waveguides. The gun pressure is expected to further decrease with an extended period of rf power processing, which is planned when gun rf operation resumes. The goal is a pressure  $< 1e-9$  Torr at nominal average power.

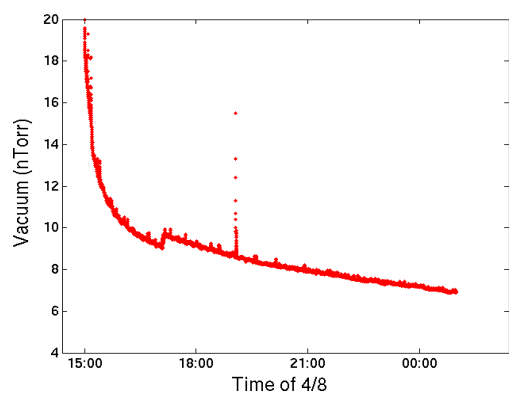


Figure 3: Gun vacuum improvement through rf power processing.

### CW Operations for the Gun and Buncher

Initial CW gun operation at nominal peak power was established with the low level (llrf) drive frequency changing to match the gun cavity frequency while ramping up the gun power and duty cycle. Then the gun mechanical tuners were adjusted to match the gun cavity frequency to the nominal frequency, 186.714 MHz (1300/7 MHz), and finally the tuner feedback switched on. Figure 4 shows one example for the manual gun turn-on process: RF peak power, duty cycle, cavity frequency detune, and gun cavity temperature evolution. The full gun turn-on process may take up to about 30 minutes when done manually. It is expected that the gun turn-on process can be further shortened after optimization and automation of the procedures.

The gun energy is measured with an rf probe installed in the gun body, based on measured rf power and cavity rf parameters. Figure 5 shows  $\sim 0.72$  MV of the gun energy is obtained with the nominal  $\sim 82$  kW peak power. The measured gun energy with the probe is very close to the expected gun energy of 0.75 MV for this power level. The electron beam-based measurement for the gun energy is planned after generating photo-electrons.

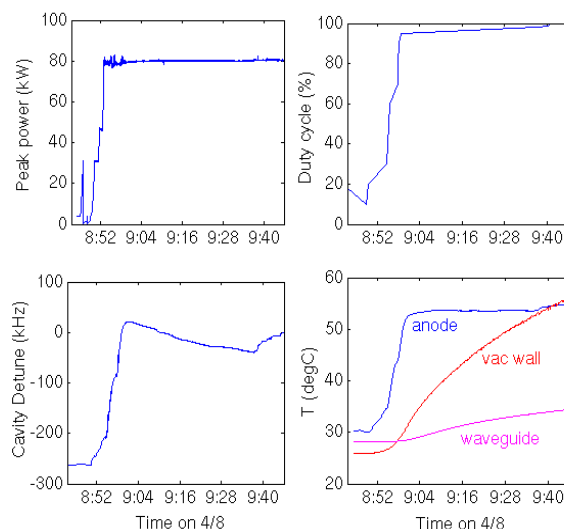


Figure 4: Gun operation ramping to nominal peak power (top left), duty cycle (top right), nominal frequency (bottom left), and gun temperature evolution (bottom right).

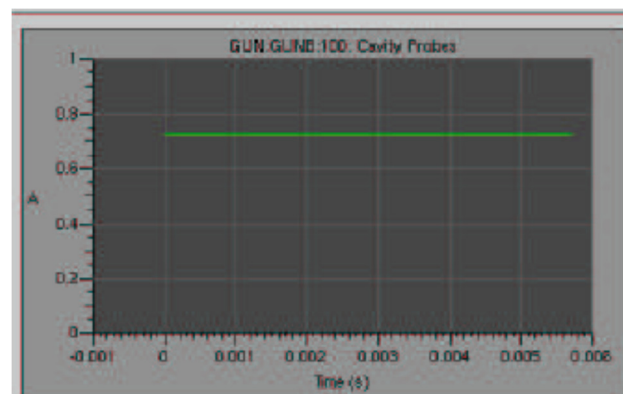


Figure 5: Gun RF probe amplitude with nominal  $\sim 80$  kW of peak power.

We also established CW operation for the buncher with nominal average power. The turn-on procedures for the buncher are similar to the gun. First, we changed llrf drive frequency to follow the buncher cavity frequency while ramping up its power and duty cycle; then changed water temperature to match the buncher cavity frequency to the nominal frequency of 1300 MHz. Figure 6 shows one example of the manual buncher turn-on process: rf peak power, duty cycle, cavity frequency. It is expected the buncher turn-on process can be completed within a few minutes only after optimization and automation of the procedures.

The buncher fields are measured with two rf probes installed in the buncher cavity body but the two measurements have some discrepancy. The next step is to understand the difference of the two probe signals and calibrate the buncher energy with electron-beam based energy measurements.

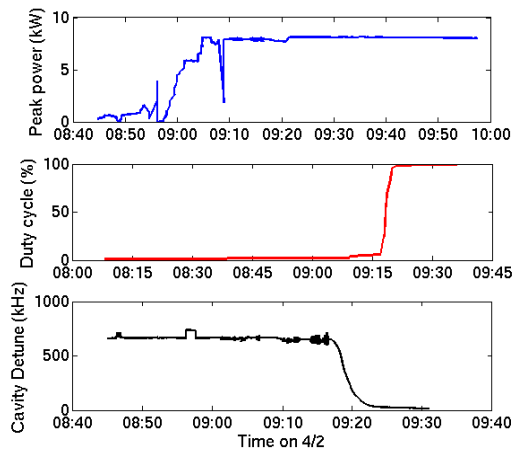


Figure 6: Buncher operation ramping to nominal peak power (top), duty cycle (middle), and nominal frequency (bottom).

### RF Jitter Measurements

We measured rf stability for both the gun and buncher. Figure 7 shows the gun in-loop rf amplitude and phase jitters with the feedback on. The amplitude jitter is  $4e-6$  rms while the phase jitter is  $0.0004^\circ$  rms. These in-loop jitters are better than the specification of  $1e-4$  rms and  $0.04^\circ$  rms for amplitude and phase jitters respectively.

Figure 8 shows the buncher out-loop rf amplitude and phase jitters. The amplitude jitter is  $7e-5$  rms while the phase jitter is  $0.1^\circ$  rms. The amplitude is within the specification of  $3e-4$  while the phase exceeds the specification of  $0.015^\circ$ . During this measurement, the buncher cavity frequency has a large detune from the nominal frequency due to water cooling issues. Figure 8 shows the phase jitter is correlated to the cavity frequency detune from the nominal frequency. The phase jitter is expected to be significantly improved when the cavity reaches the nominal frequency and feedback turned on.

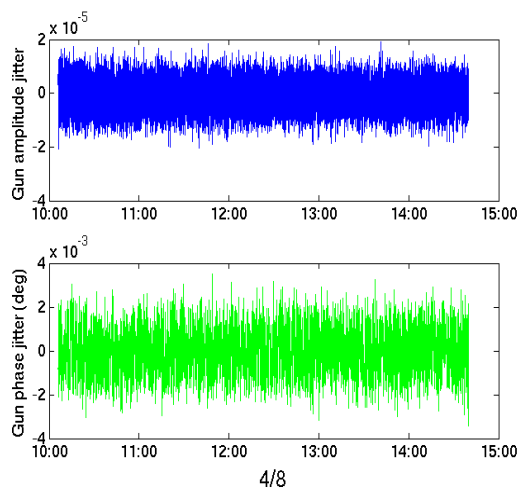


Figure 7: Gun lrf jitter for in-loop amplitude (top) and phase (bottom).

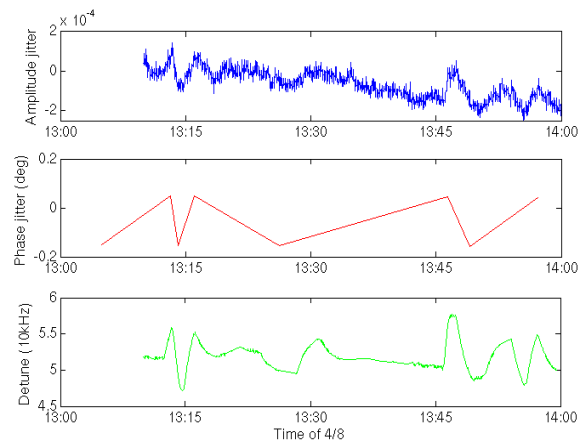


Figure 8: Buncher lrf out-loop jitter for amplitude (top), phase (middle), and cavity frequency detune from nominal (bottom).

### Dark Current Measurement

10-20 nA of dark current at the Faraday cup, much lower than the specification of 400 nA, was measured at the FC using a picoammeter with the gun operating at  $>80$  kW in CW mode. Figure 9 shows the dark current image on the YAG screen. Systematic measurement of the dark current is planned.

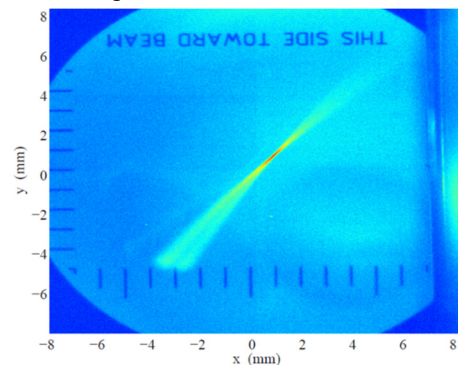


Figure 9: Example of dark current image on the YAG screen.

## SUMMARY

LCLS-II injector source commissioning has begun. So far we have improved the gun vacuum pressure, established CW gun and buncher operations, measured rf jitters and dark current while gaining CW operational experience. Next steps are to generate first photo-electron beam, measure beam energy and optimize electron beam performance.

## REFERENCES

- [1] LCLS-II Design Report, SLAC, Stanford, CA, USA, 2016. [https://docs.slac.stanford.edu/sites/pub/Publications/LCLSII%20Final\\_Design\\_Report.pdf](https://docs.slac.stanford.edu/sites/pub/Publications/LCLSII%20Final_Design_Report.pdf)
- [2] R. Wells *et al.*, *Rev. Sci. Instrum.*, vol. 87, p. 023302, 2016.
- [3] S. P. Virostek, F. Sannibale, J. W. Staples, and H. J. Qian, "The RF and Mechanical Design of a Compact, 2.5 kW, 1.3 GHz Resonant Loop Coupler for the APEX Buncher Cavity", in *Proc. 8th Int. Particle Accelerator Conf. (IPAC'17)*, Copenhagen, Denmark, May 2017, pp. 4380-4382. doi:10.18429/JACoW-IPAC2017-THPIK120